

Through Process Modelling of Self-Piercing Riveting

Porcaro, R.¹, Hanssen, A.G.^{1,2}, Langseth, M.¹, Aalberg, A.¹

¹ *Structural Impact Laboratory (SIMLab), Department of Structural Engineering, Norwegian University of Science and Technology, N-7491 Trondheim, Norway*

² *SINTEF Materials Technology, N-7465 Trondheim, Norway*

Abstract

Self-piercing riveting is a relatively new process for joining sheet metals in automotive structures. Information obtained from the riveting process simulation can lead to an improvement in the process design achieving reduction in cost and improvement in the quality of the joint. The process data can also be used to set initial parameters for a 3D simulation of the self-piercing rivet connection under combined tensile and shear loading conditions. Comparison of the results from the 3D simulation with experimental data will give a further proof of the quality of the self-piercing riveting process simulation and a better understanding of the behaviour of the connector. Such information can then lead to an improvement of a numerical model of self-piercing riveted joints using shell elements in crash analysis. In this paper, simulations of the self-piercing riveting process using LS-DYNA are presented. An implicit solution technique with r-adaptivity has been used. The advantages and the limits of using r-adaptivity in this class of metal forming process are discussed. In addition, parametric studies on important parameters for the forming process, i.e. friction, mesh size and failures criteria are presented. Finally, the mapping of data, the 3D simulation of the rivet specimen and the comparison with experimental results are presented.

Introduction

Self-piercing riveting is a relatively new process for joining sheet metals in the automotive industry. Its importance is growing because of its advantages over spot welding of aluminium alloys. Unlike the traditionally riveting process, there are no pre-drilled or pre-punched holes required in the self-piercing riveting process and there is no need for exact alignment between the sheets being joined and the rivet setting machine. Few studies have been carried out on self-piercing riveting.

A thorough study of the self-pierce riveting process was done by Hahn and Dölle [1]. An experimental test rig was established that enables force to be measured during the riveting process. Moreover, a numerical model of the riveting process was made using the finite element (FE) program MSC.AutoForge. Here, a geometric failure criterion on the minimum allowable sheet thickness was used to predict failure in the numerical model. Good agreement was found between the experimental force-deformation curves and the corresponding simulations. Fu and Mallick [2] have presented experimental data on the effect of several process parameters, such as rivet diameter, rivet length, rivet hardness, sheet thickness and die shape, on the static and fatigue properties of self-piercing riveted joints in aluminium alloy AA5754.

Accurate and reliable modelling of a self-piercing riveted connection using shell elements is a difficult task. Any improvements of such models in order to overcome the enormous simplification should be based on the physical behaviour of the connection. Going from the riveting process to a 3D model of the connection can lead to a better understanding of the physical phenomena governing this problem. Figure 1 shows the strategy and the objectives of this study.

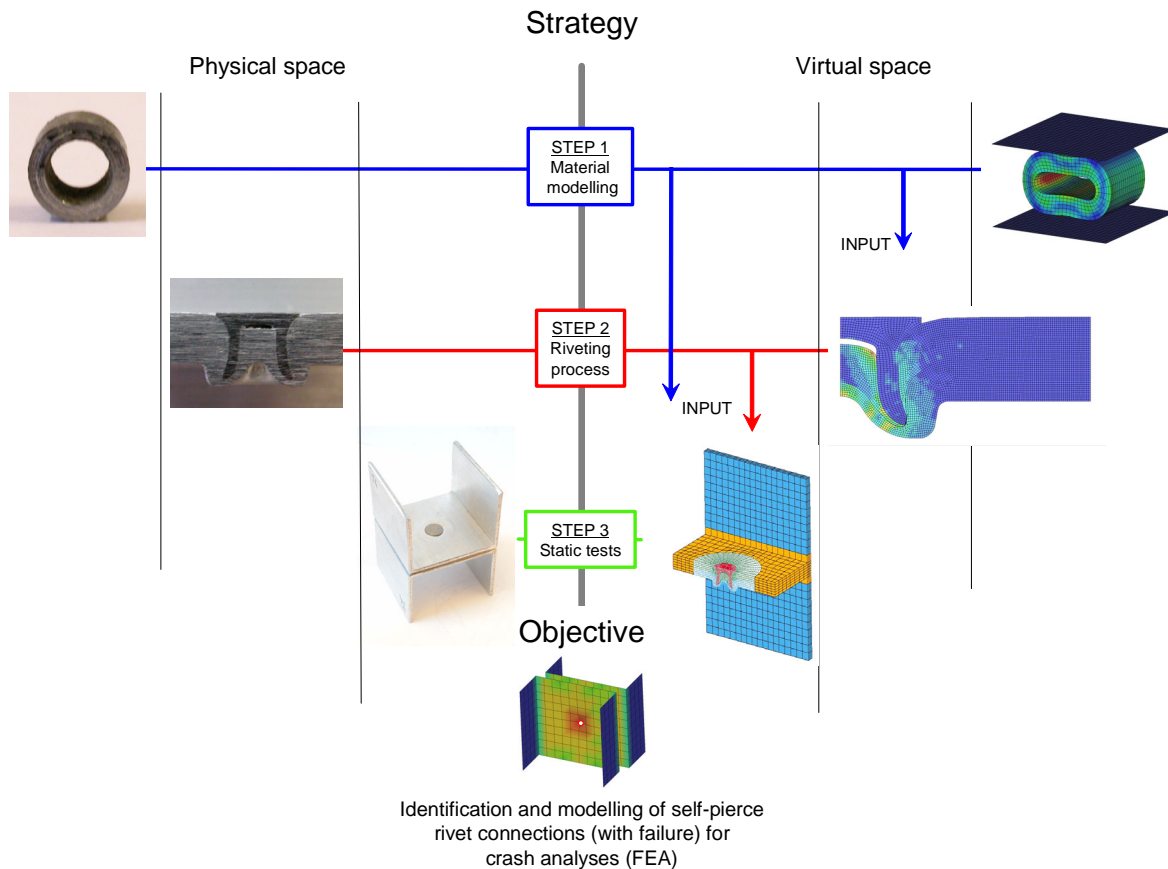


Figure 1. Objective and strategy of the project.

A numerical simulation of the self-piercing riveting process using the commercial code LS-DYNA is presented. An implicit solution technique with r-adaptivity has been used. Geometrical failure based on the change in thickness of the connected plates was used. The influence of the friction parameters and the mesh size sensitivity were investigated. A 3D model for structural analysis was generated based on the current geometry and material properties obtained from the process. Static tests were simulated using an explicit solution technique. Three different load conditions were simulated, 0° (shear), 45°, 90° (pull-out). The results were compared with experimental data.

Material properties

The specimens were made of aluminium alloy 6060 temper T4 while the rivet was made of high-strength steel. The material properties of the base material were obtained by means of uniaxial tensile tests, Figure 2a. The material properties of the rivet were obtained by inverse modelling. A cylinder was cut from the shank of the rivet and tested in lateral compression. A numerical model of the cylinder was generated using hexahedral solid elements and an elasto-plastic material, type 24 in LS-DYNA (*MAT_PIECEWISE_LINEAR_PLASTICITY). Figure 2b shows the comparison between the model and the experiments using the tabulated material data given here.

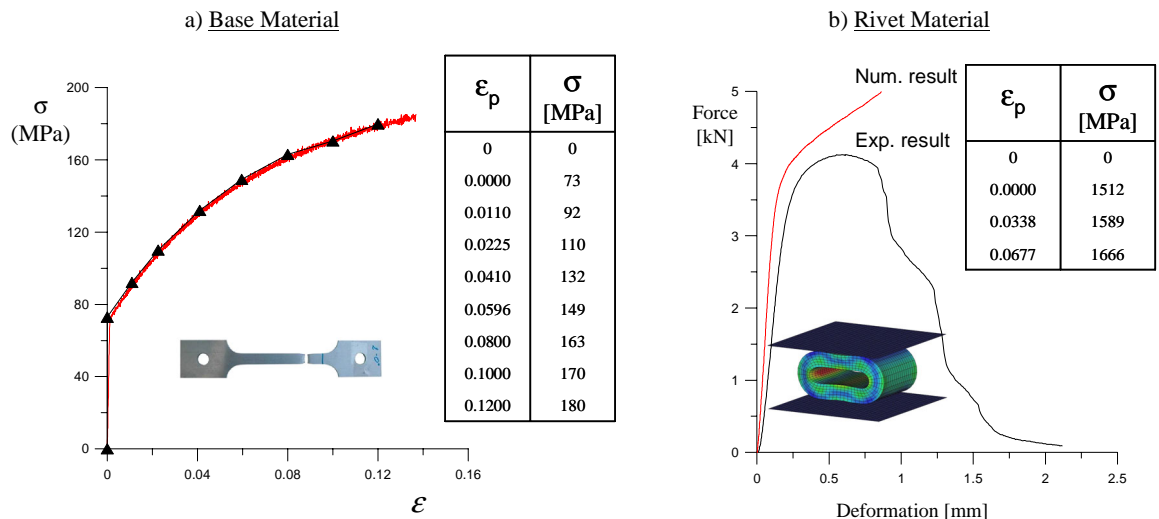


Figure 2. Material characterization: a) base material; b) rivet material.

Riveting Process

Self-piercing riveting is essentially a cold forming process, in which a semi-tubular rivet, pressed by a plunger, pierces through the thickness of the upper sheet and flares into the bottom sheet, forming a mechanical interlock between the two sheets. The self-piercing riveting process can be described by the following three steps: a) Clamping, i.e. the blank holder presses the two sheets against the die; b) Piercing, i.e. the punch pushes the rivet into the plate; and c) Flaring, i.e. the material of the lower sheet flows into the die and the rivet shank begins to flare outward, forming a mechanical interlock between the upper and lower substrates. Figure 3 shows the steps of the self-piercing riveting process.

Riveting Process Tests

A new testing device was developed at SIMLab in order to investigate the riveting process. Force-displacement histories were recorded during the tests and used to calibrate the numerical model of the riveting process. Figure 4 shows the testing device, the cross section of the final joint and a measured force-displacement curve.

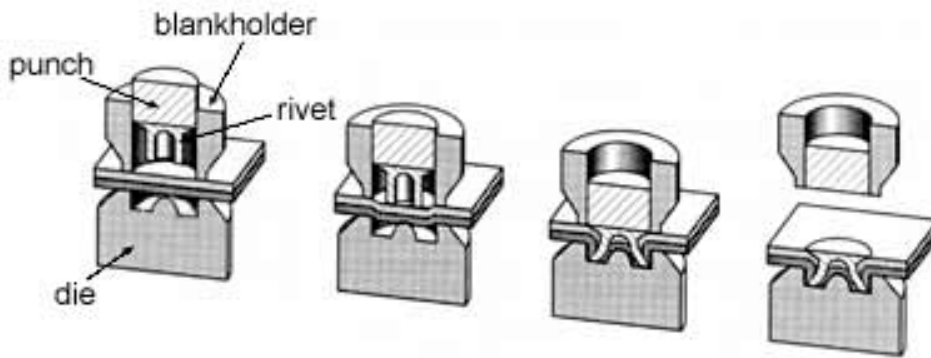


Figure 3. Self-piercing riveting process [3].

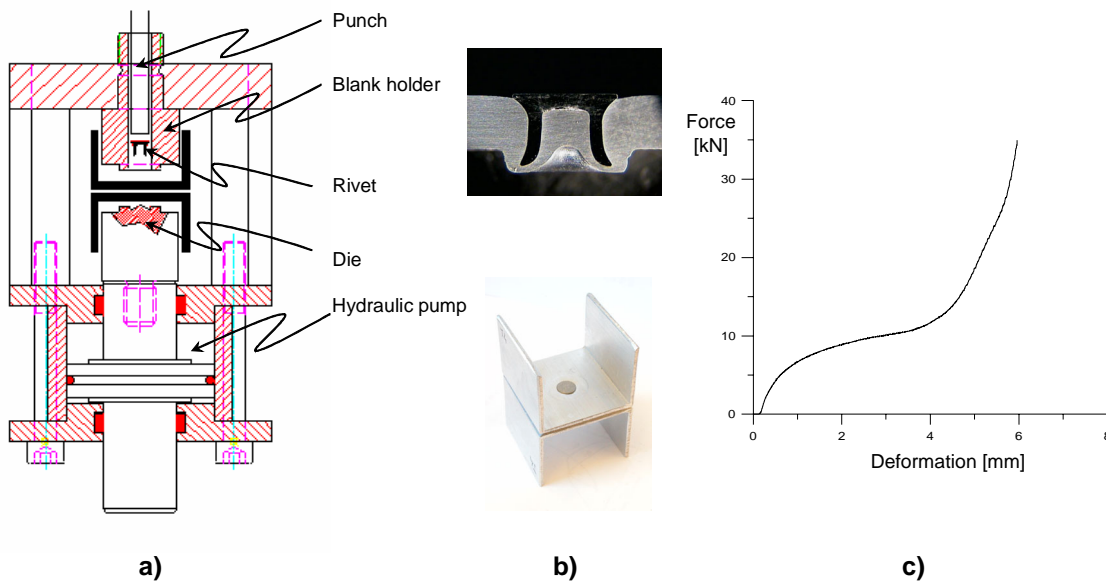


Figure 4. Self-piercing riveting process test: a) test device; b) cross section and geometry of the sample; c) force-deformation curve.

Numerical Simulation of Riveting Process

A numerical model was generated with LS-DYNA. The simulations were performed using an implicit time integrator algorithm. As the problem is axisymmetric, the 4-node 2D axisymmetric elements have been used, with four Gauss points and a stiffened based hourglass control (assumed strain co-rotational stiffness form). The size of the smallest element in both the sheets and rivet was $0.1 \times 0.1 \text{ mm}^2$. The punch, blank holder and die were modelled as rigid bodies, while the material of the rivet and the sheets were modelled as an elasto-plastic materials (*MAT_PIECEWISE_LINEAR_PLASTICITY). Contact was modelled using an automatic 2D single surface penalty formulation available in LS-DYNA. Figure 5 shows the initial configuration of the riveting process. Firstly, a displacement is prescribed for the blank holder. When the sheets are clamped between the blank holder and the die, a pressure is applied to the blank holder in order to keep the sheets tight. Secondly, a displacement is prescribed for the punch that pushes the rivet through the sheets until the joint is formed.

Self-piercing riveting process involves large strains and plastic deformations. To simulate this process it is necessary to use formulations that consider geometry changes and material non-linearity. During deformation, the elements in the mesh may become severely distorted. This may lead to a premature termination of the analysis. Using a simple erosion technique, deleting the elements when the plastic strain reaches a critical value specified by the user, does not solve the problem. The interface between the rivet and the plate will not be smooth and a premature termination of the analysis may occur due to severe distortions of the elements in front of the shank of the rivet.

In order to get a reliable solution, an adaptive meshing technique was used. In the present version of LS-DYNA two types of adaptivity methods are available, i.e. r- and h-adaptivity. For the 2D axisymmetric element, only the r-adaptivity method can be used. When using adaptivity in LS-DYNA, the user specifies a birth time, t_{birth} , at which the adaptive remeshing begins, the death time, t_{death} , at which the adaptive remeshing ends, and a time interval, Δt , between each remeshing. Alternatively, the user can define a load curve that gives the Δt as a function of time. At each remeshing interval, nodal values for all variables

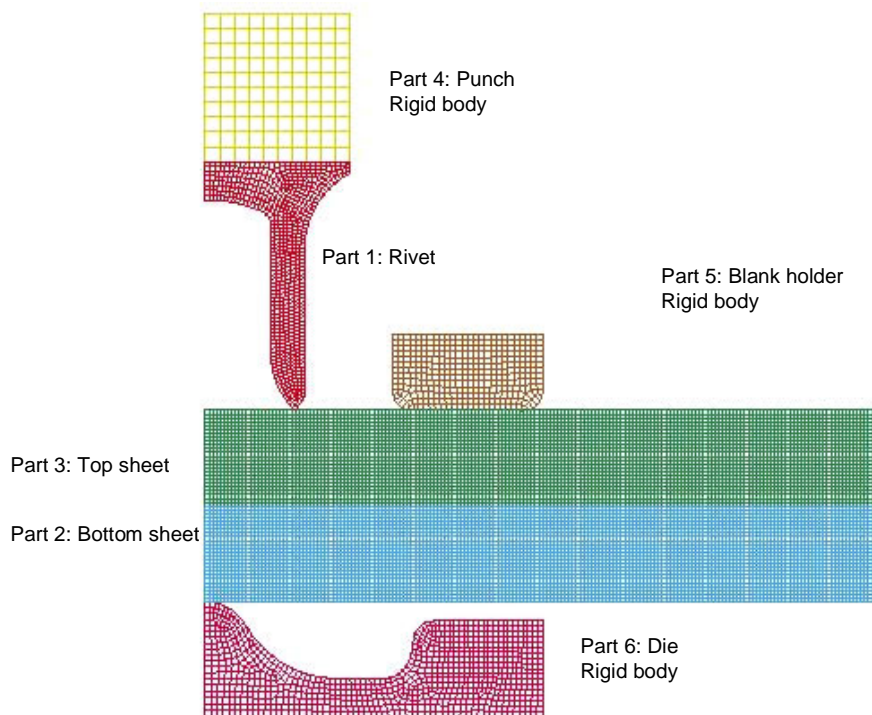


Figure 5. Geometry of the numerical model.

to be remapped are generated. A completely new mesh is generated from the old mesh, based on the characteristic element size. The new mesh is initialized from the old mesh using a least squares approximation [3-4]. 2D adaptive simulation can be combined with a failure criterion based on geometrical considerations. When the upper sheet thickness reaches a user-defined value the sheet is divided into two parts. This procedure allowed the rivet to penetrate into the bottom sheet.

The adaptivity method, used in LS-DYNA, may have disadvantages. It is not possible to remesh only the local part under the rivet shank, while keeping the rest fixed; or as some r-methods do, focusing on the region of more interest in a way to have a finer mesh where is

needed and a coarser one in the remaining regions. At each adaptive step, a completely new mesh with uniform element size is generated for all the parts selected. Failure criteria, based on erosion of elements, and an adaptivity procedure can not be used together as numerical problems will occur. During a remeshing step, if some elements have been removed, the adaptive procedure, when creating the new mesh, will still take into account the nodes that have been deleted, creating some elements that can have negative volume. This leads to an error termination of the simulation.

A mesh sensitivity study for adaptive simulations was carried out. Different combinations of mesh size and adaptive time interval were performed. As the r-adaptivity is not able to keep nodes on a smooth surface when using a high number of adaptive steps, the curvature of the borders of the sheets was approximated with a straight line giving a non physical result, Figure 6a. Reducing the adaptive time steps we can obtain a better results as shown in Figure 6b. On the other hand, when the element size increase the material under the rivet shank is not able to flow away. In the case, the rivet is stuck in the top sheet, which does not allow the opening of the rivet shank. Also the length of the rivet shank is reduced due to high compression, Figure 6c.

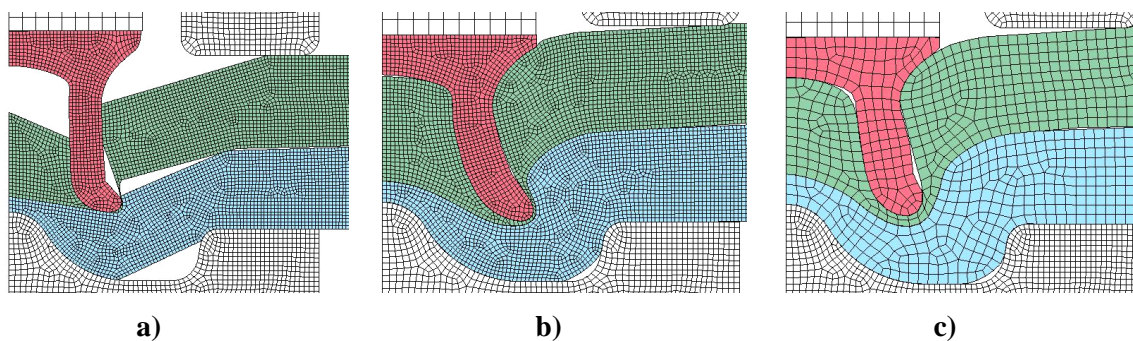


Figure 6. a) 200 adaptive steps over 250 total steps; b) 20 adaptive steps over 250 total steps; c) Mesh size 0.25mm x 0.25mm.

A mesh size of $0.1 \times 0.1 \text{ mm}^2$ was used for the parts that were adaptive remeshed as well as for remaining parts in order to reduce contact problems. The adaptive time interval value of $8 \cdot 10^{-3}$ sec, corresponding to 12 adaptive steps over a total number of 250 steps, was used. The hourglass coefficient value for the sheets was set to 0.01 while for the rivet the value was set to 0.1. The following values of the friction coefficients were used: FR=0.15 aluminium to aluminium, FR=0.3 bottom sheet to die, FR=0.3 top sheet to blank holder, FR=0.2 rivet to sheets. Figure 7 shows a visual comparison between the numerical simulation and specimen as well as a comparison between the numerical and experimental force-deformation curves from the riveting process. In the figure the borders of the numerical joint have been placed on the picture of the cross section of the specimen. Good agreement between numerical and experimental force-deformation curves was found.

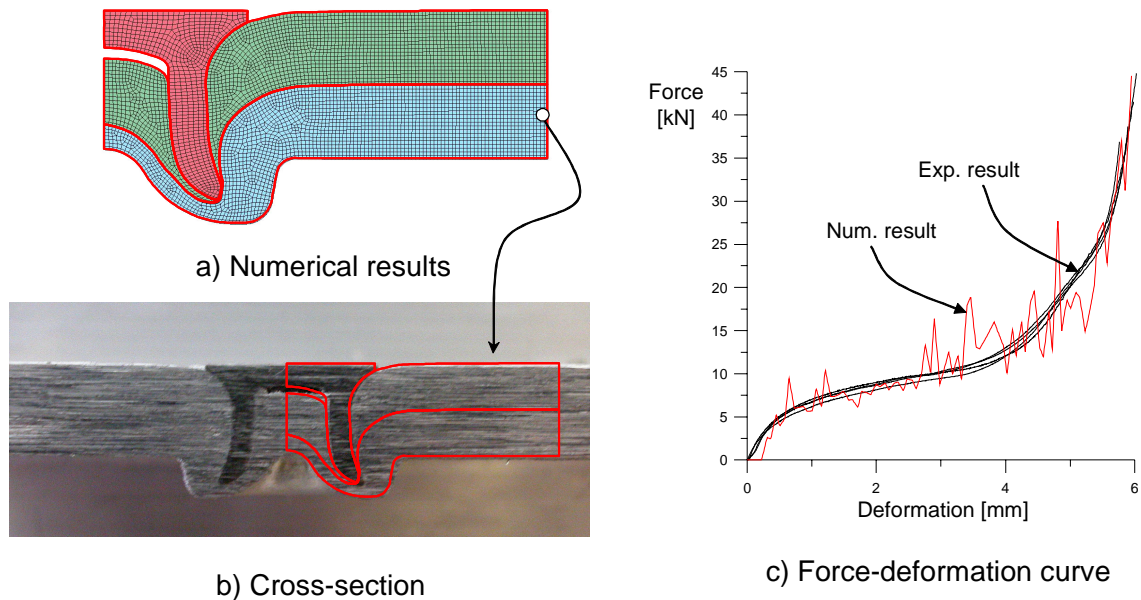


Figure 7. Comparison between simulation and test.

Single-Rivet Specimen

A quasi-static test of the single-rivet specimen, previously riveted by the testing device presented above, was carried out. The geometry of the specimen is shown in Figure 8 as well as the test fixture. This test set-up enables to investigate the structural behaviour of the connection subjected to a load combination of shear and pull-out. Three different loading conditions were investigated, 0° (shear), 45° and 90° (pull-out). Figure 8b shows the measured force-displacement curves from the tests.

A 3D numerical model of a single rivet specimen was generated to simulate the quasi-static behaviour of the connection. The model was generated based on the results of the riveting process simulation, Figure 9a. The deformed geometry and stress-strain distribution was mapped into a 3D model represented by hexahedral elements. Firstly, the new geometry was generated revolving the borders of both the rivet and the sheets around the axis of symmetry and a new mesh was generated, Figure 9b. Care was taken to get hexahedral elements in the central part (near the symmetry axis) of the model. Secondly, the stress-strain field was mapped; the average values of each integration point of the 2D elements located inside the 3D element were assigned to all the 3D elements with the same radius position. Finally, the model of the single-rivet specimen was assembled connecting the internal part, generated from the process simulation, with the external part by means of a contact algorithm, Figure 9c.

The simulations were performed using an explicit time integrator algorithm. The hexahedral element with constant stress was used together with a stiffened based hourglass control (assumed strain co-rotational stiffness form). The same material model and material parameters as used for the riveting process simulation were used. Contact was modelled using an

automatic surface-to-surface penalty formulation available in LS-DYNA. The displacement is prescribed to the flanges of the upper sheet, while the flanges of the bottom sheet were fixed. The flanges were defined as rigid bodies. Three different loading conditions were considered, 0° (shear), 45° and 90° (pull-out). Figure 10 shows the comparison between the experimental and numerical results. The comparison for the pull-out condition (90°) shows a good agreement in the first part, but the numerical curve did not reach the maximum

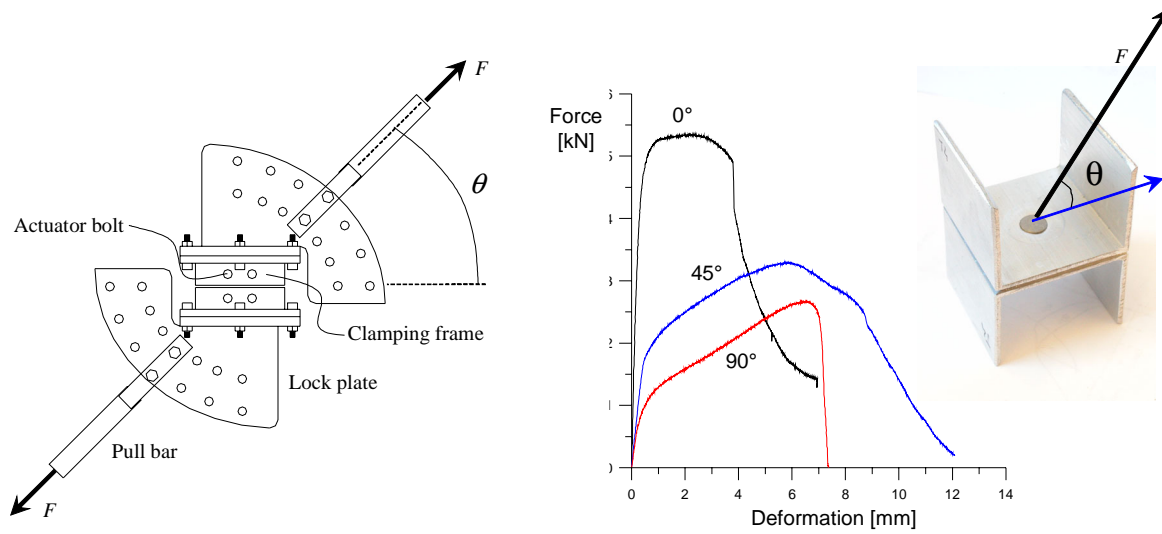


Figure 8. a) Test fixture at SIMLab; b) force-deformation curves; c) Single rivet specimen.

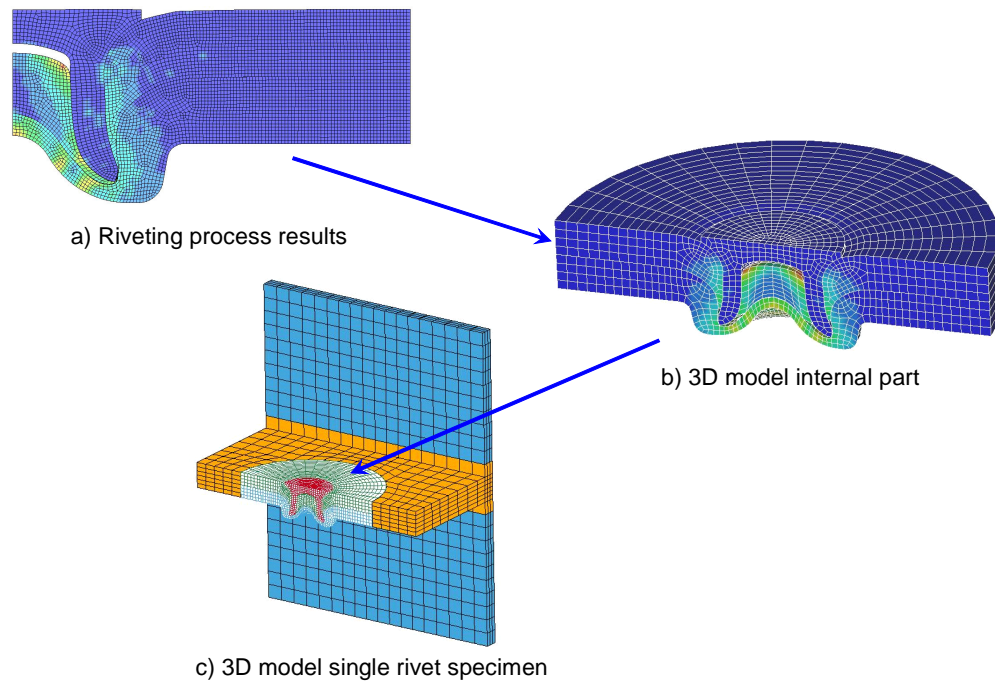


Figure 9. Geometry of the 3D simulation.

force and displacement measured during the test. This effect can be explained as lack of penetration of the rivet shank in the bottom sheet. The same behaviour can be observed also for the 45°. The results for the pure shear condition (0°) have shown a sudden reduction in the force level. This may be caused by of the insufficient contact between the shank of the rivet and the bottom sheet. Figure 10 shows also the force-deformation curves of the simulations performed without mapping the stress-strain distribution from the final configuration of the riveting process. The comparison shows a lower force level in the latter simulations.

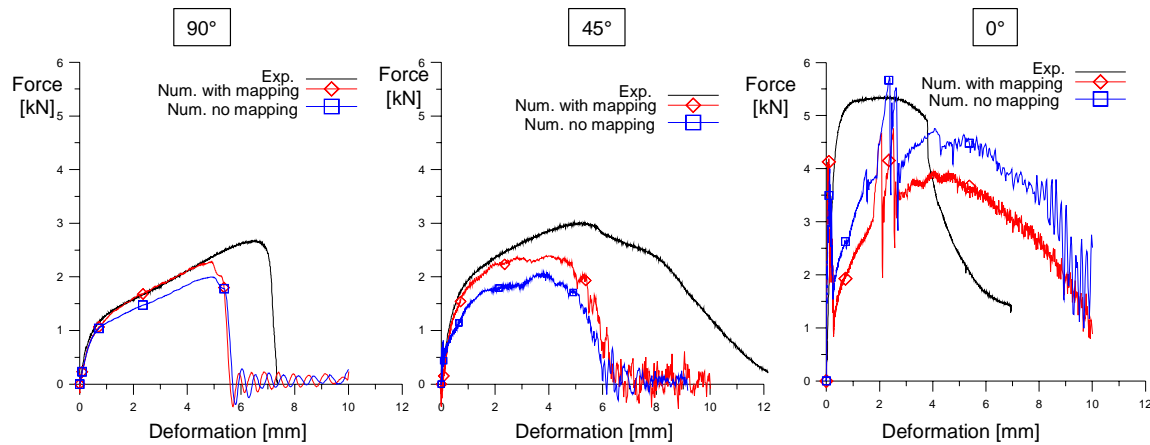


Figure 10. Comparison between experimental and numerical force-deformation curves.

Conclusions

Self-piercing riveting is a relatively new process for joining sheet metals in the automotive industries. A through process modelling of self-piercing riveting has been presented. Numerical simulations of the self-piercing riveting process have been carried out using the commercial code LS-DYNA. An implicit solution technique together with an r-adaptive method has been used. The influence of the most important parameters for such type of simulations has been investigated, i.e. friction, mesh size and time adaptive interval. A new test device has been developed for measurement the force-deformation history during the riveting process. Good agreement between the simulation and the test has been found.

The final configuration from the process simulation has been mapped into a 3D model of a self-piercing rivet connection using hexahedral elements. Static test with different combination of the loading condition have been simulated. The importance of mapping the stress-strain distribution in order to get the correct force-deformation level has been shown. The model is able to capture the physical failure mechanisms of the connection, but further research is required in order to improve the performance of the model.

Reference

- [1] O. Hahn and N. Dölle: "Numerische Simulation des Fügeprozesses beim Stanznieten mit Halbhohlniet von duktilen Blechwerkstoffen. Universität Paderborn", LWF Schriftreihe 48. Shaker Verlag, Aachen. ISBN3-8265-9427-4 (2001).
- [2] Fu M. and Malick P.K., "Effect of process variables on the static and fatigue properties of self-piercing riveted joints in aluminium alloy 5754", Society of Automotive Engineers, SAE Paper No. 2001-01-0825, 2001.
- [3] The Welding Institute TWI. www.twi.co.uk.
- [4] Hallquist J.O. LS-Dyna Theoretical Manual. Livermore Software Technology Corporation (1998).
- [5] Livermore Software, LS-Dyna Keyword users Manual, version 970. Livermore Software Technology (2003).